Galectin-3 regulates myofibroblast activation and hepatic fibrosis

Neil C. Henderson*, Alison C. Mackinnon*, Sarah L. Farnworth*, Francoise Poirier†, Francesco P. Russo*, John P. Iredale*, Christopher Haslett*, Kenneth J. Simpson*, and Tariq Sethi*‡

*Centre for Inflammation Research, Queens Medical Research Institute, University of Edinburgh, 51 Little France Crescent, EH16 4SA Edinburgh, Scotland, United Kingdom; and †Laboratoire de Genetique et Developpement des Mammiferes, Institut Jacques Monod, 2, Place Jussieu, 75251 Paris Cedex 05, France

Central to fibrogenesis and the scarring of organs is the activation of fibroblasts into matrix-secreting myofibroblasts. We demonstrate that Galectin-3 expression is up-regulated in established human fibrotic liver disease and is temporally and spatially related to the induction and resolution of experimental hepatic fibrosis. Disruption of the *Galectin-3* gene blocks myofibroblast activation and procollagen (I) expression *in vitro* and *in vivo*, markedly attenuating liver fibrosis. Addition of exogenous recombinant Galectin-3 *in vitro* reversed this abnormality. The reduction in hepatic fibrosis observed in the *Galectin-3*$^{-/-}$ mouse occurred despite equivalent liver injury and inflammation, and similar tissue expression of TGF-β. TGF-β failed to transactivate *Galectin-3*$^{-/-}$ hepatic stellate cells, in contrast with WT hepatic stellate cells; however, TGF-β-stimulated Smad-2 and -3 activation was equivalent. These data suggest that Galectin-3 is required for TGF-β mediated myofibroblast activation and matrix production. Finally, *in vivo* siRNA knockdown of Galectin-3 inhibited myofibroblast activation after hepatic injury and may therefore provide an alternative therapeutic approach to the prevention and treatment of liver fibrosis.

hepatic stellate cell | liver | small interfering RNA | TGF-β

Fibrosis represents the final common pathway of chronic tissue injury. Chronic inflammation with the formation of scar tissue, loss of tissue architecture, and organ failure is a characteristic feature of the pathogenesis of many human diseases and represents a major cause of morbidity and mortality worldwide. Currently our therapeutic repertoire is limited to immunosuppression and/or organ transplantation (1, 2). Therefore, effective alternative therapies are urgently required.

The fibroblast and myofibroblast are key cells in the initiation and perpetuation of organ scarring (3, 4). Classically, quiescent tissue fibroblasts become activated to a contractile, myofibroblast matrix-secreting phenotype. Understanding the molecular mechanisms that drive this phenotype switch may allow the development of targeted antifibrotic therapies.

Galectins are members of a growing family of animal lectins (5–8). Galectin-3 is a β-galactoside-binding animal lectin of $\approx$30 kDa. This unique Galectin is composed of two domains: a carboxyl-terminal domain that contains the carbohydrate-binding region and an amino-terminal domain consisting primarily of tandem repeats of nine amino acids (9) to cross-link carbohydrate and noncarbohydrate ligands. Galectin-3 is a pleiotropic molecule found in the nucleus, cytoplasm, and at the cell surface and can also be secreted by an unorthodox mechanism that bypasses the endoplasmic reticulum and the Golgi apparatus (10). *In vitro* Galectin-3 has been implicated in a variety of biological processes including cell proliferation (11, 12), adhesion (13–15), and survival (16, 17). Initial *in vivo* studies demonstrated that Galectin-3 knockout mice have attenuated peritoneal inflammatory responses to thioglycollate instillation (18, 19), suggesting a role for Galectin-3 in the development of acute inflammation. However, the mechanisms that are involved in fibrogenesis are distinct from those involved in inflammation (20). Increased Galectin-3 expression has been noted in

tissue fibrosis (21–23), and *in vitro* exogenous Galectin-3 stimulates myofibroblast proliferation (24, 25). The relevance of these observations to the mechanistic role of Galectin-3 in the pathogenesis of tissue fibrosis *in vivo* has not been examined. We therefore examined myofibroblast activation and collagen deposition in an experimental model of hepatic fibrosis by using mutant mice lacking the *Galectin-3* gene.

Results

Galectin-3 Expression Is Up-Regulated in Human Liver Fibrosis and Is Temporally and Spatially Related to Fibrosis in a Reversible Rat Model of Liver Fibrosis. In established human liver fibrosis, regardless of etiology (hepatitis B or C, autoimmune, copper or iron overload, primary biliary cirrhosis, or alcohol-induced), Galectin-3 expression was negligible in normal liver and dramatically increased in the cirrhotic nodules of hepatocytes, particularly at the periphery of the nodules ($n = 36$ cases) (Fig. 1 *a* and *b*). Furthermore, Galectin-3 expression was examined in a well established rat model of reversible carbon tetrachloride (CCL$_4$)-induced liver fibrosis (26, 27) (Fig. 1*c*). Galectin-3 expression was temporally and spatially associated with fibrosis [collagen fibers stained red with picrosirius red (PSR)], minimal in normal rat liver, maximal at peak fibrosis, and was virtually absent again at 24 weeks (recovery from fibrosis). This finding suggests that the development (and resolution) of fibrosis may be regulated by Galectin-3.

Galectin-3 Plays a Critical Role in Liver Fibrosis. The significance of the above observations was examined by using CCL$_4$-induced liver injury as a model system for liver fibrogenesis. After 8 weeks of CCL$_4$ treatment, increased Galectin-3 expression was observed in the periportal areas and areas of bridging fibrosis in the liver. Dense Galectin-3 staining was noted at the periphery of the inflamed damaged areas. Galectin-3 was only expressed in bile duct epithelia and Kupffer cells in the liver from control (olive oil treated) animals (Fig. 2*a*). A marked increase in Galectin-3 mRNA (real-time PCR) and protein expression (Western blot analysis) was demonstrated with the development of hepatic fibrosis in the CCL$_4$-treated animals compared with control (Fig. 2*b*). Hepatic collagen was stained with PSR (Fig. 2*c*) and quantified by using digital image analysis (Fig. 2*d Left*). Striking collagen deposition in the same distribution as Galectin-3 was present in the periportal areas and areas of bridging fibrosis in the WT animals. By contrast, there was significantly less collagen deposition in the *Galectin-3*$^{-/-}$ mice ($P < 0.05$). Procollagen (I) mRNA expression [collagen (I) is highly expressed in human and animal models of liver fibrosis] was significantly decreased in the livers from *Galectin-3*$^{-/-}$ compared with WT mice after chronic CCL$_4$ treatment as judged by real-time PCR ($P < 0.05$) (Fig. 2*d*

Fig. 1. Galectin-3 expression is up-regulated in human liver fibrosis. (*a*) Galectin-3 expression in normal human liver. (*b*) Galectin-3 in cirrhosis secondary to hepatitis C infection. (Scale bar: 400 μm.) Galectin-3 expression is temporally and spatially related to fibrosis in a reversible rat model of liver fibrosis. (*c Upper*) Collagen stained with PSR. (Scale bar: 100 μm.) (*c Lower*) Galectin-3 immunohistochemistry. (Scale bar: 200 μm.) (*Left*) Control (olive oil vehicle only). (*Middle*) Peak fibrosis in rat liver after 12 weeks of twice weekly i.p. CCL$_4$. (*Right*) Resolution, 24 weeks after cessation of CCL$_4$-induced liver injury .

Right), suggesting that Galectin-3 regulates hepatic collagen deposition during liver injury. We therefore went on to examine the mechanism underlying this important observation.

The hepatic stellate cell (HSC) is the key fibrogenic cell of the liver and represents a paradigm cell type in studies of the pathogenesis of tissue fibrosis (3, 4, 28). After any cause of liver injury, quiescent HSCs undergo activation to proliferative, fibrogenic, and contractile myofibroblasts with increased expression of α-smooth muscle actin (α-SMA), a widely accepted marker of myofibroblast activation (3, 4) *in vitro* and *in vivo*. After 8 weeks of CCL$_4$ administration, α-SMA expression was markedly increased in WT compared with *Galectin-3$^{-/-}$* mice with the same temporal and spatial distribution as Galectin-3 and collagen expression (Fig. 2*e*). There was significantly less α-SMA expression in the *Galectin-3$^{-/-}$* mice compared with WT quantified by using digital image analysis (Fig. 2*f Left*; $P < 0.01$). The transcripts for α-SMA mRNA, as assessed by real-time PCR, were significantly increased in WT animals after CCL$_4$ treatment compared with animals that received olive oil (control) (Fig. 2*f Right*). However α-SMA transcripts were significantly decreased in *Galectin-3$^{-/-}$* mice compared with WT ($P < 0.01$). This decrease in mRNA expression was paralleled by a decrease in hepatic α-SMA protein expression assessed by Western blot analysis of whole liver tissue (Fig. 2*f Right Inset*). These data indicate that Galectin-3 mediated activation of HSCs *in vivo* is a central mechanism underlying hepatic fibrosis. Furthermore, we investigated myofibroblast activation in models of renal fibrosis and pulmonary fibrosis by using unilateral ureteric obstruction and intratracheal instillation of silica respectively (N.C.H. and T.S., unpublished observations). In both instances, we found defective myofibroblast activation in the *Galectin-3$^{-/-}$* mice. This finding demonstrates the broad applicability of our results and potential relevance to many forms of tissue fibrosis in different disease states.

Disruption of the Galectin-3 Gene Does Not Affect Initial Liver Injury or Inflammatory Cell Infiltrate After CCL$_4$ Treatment. After a single i.p. injection of CCL$_4$, initial hepatic injury as judged by alanine aminotransferase (a marker of hepatocyte damage) was similar in WT and *Galectin-3$^{-/-}$* mice at days 1–7 (Fig. 6 *a* and *b*, which is published as supporting information on the PNAS web site). Furthermore, total liver tissue levels of the proinflammatory cyto-

Fig. 2. Galectin-3 plays a critical role in organ fibrosis. Mice were treated with olive oil (control) or CCL$_4$ i.p. twice weekly for 8 weeks ($n = 6$ mice in each group). (*a*) Galectin-3 expression in control (*Left*) and after chronic CCL$_4$ treatment (*Right*) in WT mouse liver. (Scale bar: 400 μm.) (*b Left*) Real-time PCR quantitation of Galectin-3 expression in whole liver homogenates from control (olive oil vehicle) and chronic CCL$_4$ treated mice. ***, $P < 0.0001$ compared with control. (*b Right*) Representative Galectin-3 and β-actin Western blots of whole liver from control and CCL$_4$-treated WT mice. (*c*) Collagen staining with PSR of liver tissue after chronic CCL$_4$ treatment of WT and *Galectin-3$^{-/-}$* mice. (Scale bar: 200 μm.) (*d Left*) Digital image analysis quantification of collagen staining. *, $P < 0.05$. (*d Right*) Real-time PCR quantification of procollagen (I) mRNA in whole liver homogenates from chronic CCL$_4$ and control groups. *, $P < 0.05$ compared with WT. (*e*) α-SMA staining of liver tissue after chronic CCL$_4$ treatment. (Scale bar: 200 μm.) (*f Left*) Digital image analysis quantification of α-SMA staining. **, $P < 0.01$ compared with WT. (*f Right*) Real-time PCR quantification of α-SMA in whole liver homogenates in chronic CCL$_4$ and control groups. *, $P < 0.05$ compared with WT. (*f Inset*) Representative Western blots of α-SMA and β-actin expression in whole liver homogenates from chronic CCL$_4$-treated mice.

kine TNF-α in WT and *Galectin-3*$^{-/-}$ mice measured by ELISA were not significantly different 24 h post-CCL$_4$ liver injury (WT, 1.4 ± 0.22 ng TNF-α per μg whole liver protein; *Galectin-3*$^{-/-}$, 1.65 ± 0.3 ng TNF-α per μg whole liver protein (P value was not significant). Hepatic inflammatory cell recruitment was similar in WT and *Galectin-3*$^{-/-}$ mice at days 1–7 (Fig. 6 *c* and *d*). Furthermore, there was no difference in T lymphocyte recruitment between WT and *Galectin-3*$^{-/-}$ mice as assessed by cluster of differentiation molecule 3 (CD3) immunohistochemistry and counting. The macrophage in particular is an important inflammatory cell involved in the pathogenesis of tissue fibrosis (29, 30) and therefore we examined proinflammatory cytokine release from WT and *Galectin-3*$^{-/-}$ bone marrow-derived macrophages (BMDMs) (see *Supporting Materials and Methods*, which is published as supporting information on the PNAS web site). Maturation of WT and *Galectin-3*$^{-/-}$ BMDMs demonstrated equivalent expression of CD11b and F4/80 (Fig. 6*e*). After activation with IFN-γ/LPS, no significant difference was observed in the release of the proinflammatory cytokines TNF-α or IL-6 between WT and *Galectin-3*$^{-/-}$ macrophages (Fig. 6*f*). These data demonstrate that the difference in liver fibrosis observed between the two genotypes is not secondary to a difference in initial tissue injury, inflammatory cell recruitment, or macrophage proinflammatory cytokine release.

Myofibroblast Activation is Galectin-3 Dependent. HSC activation to a myofibroblast phenotype is a critical event in extracellular matrix deposition and cirrhosis (3, 4). We observed dual staining of Galectin-3 and α-SMA within cells in areas of fibrotic liver injury after 8 weeks of CCL$_4$ treatment in WT mice. This finding demonstrates that Galectin-3 expression is up-regulated in myofibroblasts during the injury response *in vivo* (Fig. 3*a*). Galectin-3 expression was up-regulated during myofibroblast activation *in vitro* on tissue culture plastic in both primary murine and human HSCs (Fig. 3*b*). This well-established *in vitro* method of HSC activation closely models *in vivo* myofibroblast activation (26, 27) and has been used extensively to model and examine the changes that take place during the phenotype switch of fibroblasts to extracellular matrix secreting contractile myofibroblasts. After 7 days *in vitro* culture, protein expression of α-SMA was significantly decreased in *Galectin-3*$^{-/-}$ HSCs compared with WT HSCs (Fig. 3*c*). Addition of exogenous recombinant murine Galectin-3 to *Galectin-3*$^{-/-}$ HSCs *in vitro* reversed the *Galectin-3*$^{-/-}$ phenotype resulting in increased α-SMA expression (Fig. 3*d*). Rescue of the profibrotic phenotype by exogenous Galectin-3 was confirmed with real-time PCR, which demonstrated up-regulation of procollagen (I) expression (Fig. 3*e*; $P < 0.05$). When plated on tissue culture plastic, *ex vivo* WT primary murine HSCs proliferate faster than *Galectin-3*$^{-/-}$ HSCs as judged by 3-(4,5-dimethylthiazol-2-yl)-2,5-diphenyl tetrazolium bromide assay. This defect in proliferation of the *Galectin-3*$^{-/-}$ HSCs could be restored by the addition of recombinant murine Galectin-3 (Fig. 3*f*). Fig. 3*g* shows that Galectin-3 is rapidly internalized (within 10 min) when added to *Galectin-3*$^{-/-}$ HSCs, and very little Galectin-3 accumulates at the membrane.

A rationally designed siRNA pool targeting Galectin-3 mRNA was used to inhibit Galectin-3 expression in WT primary murine HSCs. HSCs were isolated, activated on tissue culture plastic, and treated with PBS (PBS), liposome formulated nontargeted control duplex (CD), or liposome-formulated Galectin-3 siRNA. Galectin-3 siRNA treatment reduced Galectin-3 mRNA expression 10-fold as compared with control siRNA or mock treatment as assessed by quantitative real-time PCR (Fig. 4*a*; $P < 0.0001$). siRNA knockdown of Galectin-3 in HSCs did not affect cell viability assessed by trypan blue exclusion or rates of apoptosis measured by cell morphology and counting. This marked inhibition of Galectin-3 expression resulted in a significant reduction in both α-SMA and procollagen (I) mRNA expression assessed by real-time PCR (Fig. 4 *b* and *c*, respectively). Western blot analysis confirmed almost complete inhibition of Galectin-3
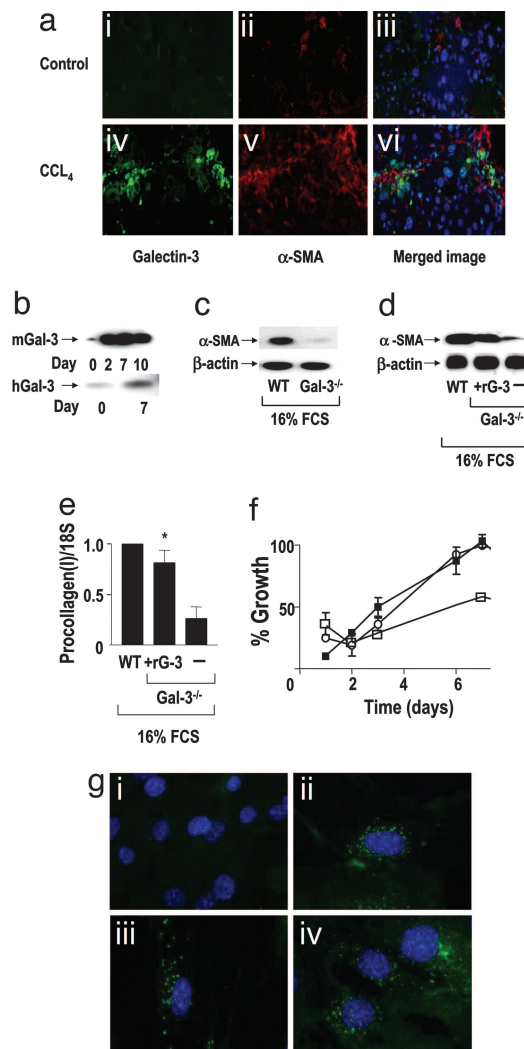
Fig. 3. Myofibroblast activation is Galectin-3 dependent. (*a*) Galectin-3 expression is up-regulated in myofibroblasts during the hepatic fibrotic response *in vivo*. Liver sections from WT control (olive oil) (*i–iii*) and chronic CCL$_4$ injured (8 weeks) (*iv–vi*) mice were stained with Galectin-3 antibody (green), anti-αSMA (red), and DAPI (blue). (*b*) Western blot analysis of Galectin-3 expression in primary mouse (mGal-3) and primary human (hGal-3) HSCs during transition from the quiescent to the activated phenotype on tissue culture plastic. (*c*) Western blot analysis of α-SMA and β-actin expression in WT and *Galectin-3*$^{-/-}$ primary mouse HSCs cultured on tissue culture plastic for 7 days in 16% FCS. (*d*) Western blot analysis of α-SMA in WT and *Galectin-3*$^{-/-}$ primary mouse HSCs after addition of recombinant murine Galectin-3 (30 μg/ml) to *Galectin-3*$^{-/-}$ HSCs in 16% FCS. (*e*) Real-time PCR quantitation of procollagen (I) in WT and *Galectin-3*$^{-/-}$ primary mouse HSCs after addition of recombinant murine Galectin-3 (30 μg/ml) in 16% FCS. *, $P < 0.05$ compared with untreated *Galectin-3*$^{-/-}$ HSCs. (*f*) Cell growth of WT (○), *Galectin-3*$^{-/-}$ (□), and *Galectin-3*$^{-/-}$ HSCs plus recombinant murine Galectin-3 (30 μg/ml) (■) measured by 3-(4,5-dimethylthiazol-2-yl)-2,5-diphenyl tetrazolium bromide assay. (*g*) Internalization of recombinant murine Galectin-3 by *Galectin-3*$^{-/-}$ primary mouse HSCs. Cells were stained with DAPI (blue) and Galectin-3 antibody (green). (*i*) Untreated, (*ii*) 10 min, (*iii*) 30 min, (*iv*) 60 min after addition of 30 μg/ml recombinant mouse Galectin-3.

expression after targeted siRNA treatment relative to control treatments (Fig. 4*d Top*). Western blot analysis also confirmed the reduction in α-SMA protein expression (Fig. 4*d Middle*). These effects were verified by using four independent murine Galectin-3 targeting siRNA duplexes (as listed in *Supporting Materials and Methods*). To assess the potential clinical applicability of Galectin-3 siRNA as a therapy in human fibrotic liver
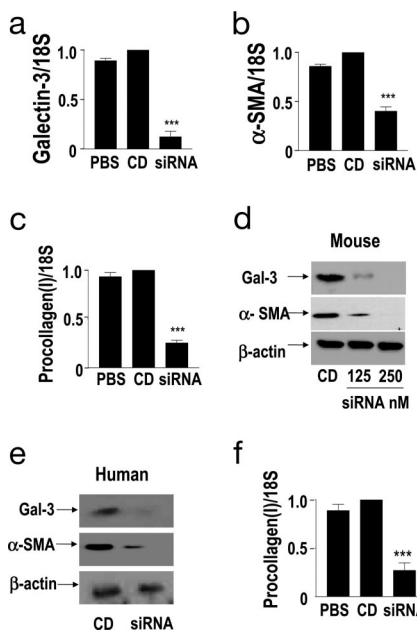
Fig. 4. Galectin-3 siRNA inhibits myofibroblast activation and procollagen (I) expression in HSCs. Real-time PCR quantitation of (*a*) Galectin-3, (*b*) α-SMA, and (*c*) procollagen (I) expression in PBS, control duplex (CD), or Galectin-3 siRNA (250 nM) treated primary mouse HSCs. ∗∗∗, *P* < 0.0001 compared with CD. (*d*) Western blot analysis of Galectin-3, α-SMA, and β-actin expression in primary mouse HSCs 96 h posttransfection. (*e*) Western blot analysis of Galectin-3, α-SMA, and β-actin expression in primary human HSCs 96 h after treatment with CD or Galectin-3 siRNA (siRNA). (*f*) Real-time PCR quantitation of procollagen (I) expression in primary human HSCs 96 h after treatment with either PBS, CD, or Galectin-3 siRNA (siRNA). ∗∗∗, *P* < 0.0001 compared with CD.

disease, primary human HSCs were transfected with human Galectin-3 targeting siRNA duplexes. Western blot analysis again showed a marked inhibition of Galectin-3 and α-SMA expression (Fig. 4*e*), and real-time PCR demonstrated a reduction in mRNA transcripts for procollagen (I) (Fig. 4*f*). These data support our *in vivo* findings that defective myofibroblast activation is the mechanism mediating reduced hepatic fibrosis observed in the *Galectin-3*⁻/⁻ mouse.

Disruption of the *Galectin-3* Gene Does Not Affect TGF-β Expression and Smad Signaling. TGF-β is a major profibrogenic cytokine involved in the pathogenesis of fibrosis in many different organ systems (31–33). However, mechanisms of tissue fibrosis also exist that are TGF-β independent, both in the liver and other organs (34, 35). The tissue expression of TGF-β mRNA is markedly elevated as judged by real-time quantitative PCR in whole liver samples after chronic CCl₄ liver injury compared with control (Fig. 7*a*, which is published as supporting information on the PNAS web site). However, there was no significant difference in hepatic TGF-β mRNA expression between WT and *Galectin-3*⁻/⁻ mice in our model of liver fibrosis (Fig. 7*a*). ELISA demonstrated no difference in the levels of TGF-β expression in WT and *Galectin-3*⁻/⁻ macrophages and HSCs in tissue culture (Fig. 7 *b* and *c*). Thus disruption of the *Galectin-3* gene blocks fibrosis despite similar expression levels of TGF-β. In the presence of TGF-β ligand, the receptor-activated Smad family of transcriptional activators, Smad-2 and -3, are phosphorylated directly by the TGF-β receptor I kinase (36). TGF-β stimulated a similar increase in Smad-2 and Smad-3 phosphorylation in WT and *Galectin-3*⁻/⁻ HSCs (Fig. 7*d*).

Addition of exogenous Galectin-3, in the presence of 16% FCS, to *Galectin-3*⁻/⁻ HSCs induced expression of α-SMA and procollagen (I) (Fig. 3). To address specifically the contribution of TGF-β to this observation, we repeated the experiments in serum-free
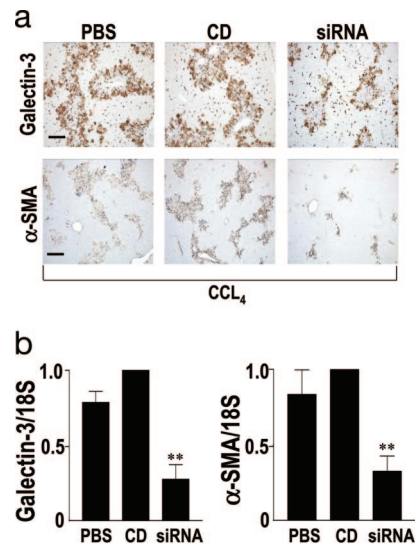
Fig. 5. Galectin-3 SiRNA-mediated inhibition of HSC activation *in vivo*. (*a*) Galectin-3 and α-SMA staining of liver tissue harvested 3 days after CCl₄ injury (*n* = 6 mice in each group). Mice received saline (PBS), control duplex (CD), or Galectin-3 siRNA (siRNA). (Scale bar: 200 μm.) (*b Left*) Real-time PCR quantitation of Galectin-3 expression in liver homogenates 3 days after CCl₄ injury. ∗∗, *P* < 0.01 compared with CD. (*b Right*) Real-time PCR analysis of α-SMA expression in liver homogenates 3 days after CCl₄ injury. ∗∗, *P* < 0.01 compared with CD.

media augmented with TGF-β (5 ng/ml). The *Galectin-3*⁻/⁻ HSCs still exhibited a reduced activation profile in the presence of TGF-β compared with WT HSCs, as demonstrated by Western blotting for α-SMA (Fig. 7*e*) and real-time PCR quantitation of α-SMA (Fig. 7*f*) and procollagen(I) (*P* < 0.0001) (Fig. 7*g*). Exogenous recombinant Galectin-3 rescued this defect in *Galectin-3*⁻/⁻ HSCs, stimulating an activated WT morphology and α-SMA filament organization (Fig. 7*h*). Western blotting for α-SMA (Fig. 7*i*) and real-time PCR quantitation of mRNA transcripts for α-SMA (Fig. 7*j*) and procollagen (I) (Fig. 7*k*) (*P* < 0.0001) confirmed the morphological changes observed. No difference was seen in either β1 integrin expression or adhesion between WT and *Galectin-3*⁻/⁻ HSCs (data not shown). Thus, Galectin-3 is essential for TGF-β-driven myofibroblast activation. Maeda *et al.* (24) suggested that Galectin-3 dependent extracellular signal-regulated kinase 1/2 (ERK1/2) activation in HSCs was PKC dependent by using a pharmacological inhibitor of PKC. However, we demonstrated no difference in the activation of PKC and ERK1/2 in response to PDGF-BB in WT, *Galectin-3*⁻/⁻ (and knockdown with siRNA) HSCs (Fig. 7*l*).

Galectin-3 siRNA-Mediated Inhibition of HSC Activation *in Vivo*. After acute CCl₄ liver injury, HSC activation peaks at day 3 and then resolves over the next 4 days. Galectin-3 siRNA was administered locally via the portal vein 2 h after CCl₄ i.p. injection. Further injections of siRNA were given hydrodynamically at 24 and 48 h. Animals were killed at 72 h to assess Galectin-3 expression and HSC activation. CCl₄ resulted in equivalent liver injury throughout all treatment groups as judged by histology, inflammatory cell infiltrate, and serum alanine aminotransferase (results not shown). Chemically modified siRNA (siSTABLE; Dharmacon Research, Lafayette, CO) was used for this study as standard siRNA is rapidly degraded by nucleases present in blood and biological fluids. Efficiency of knockdown of Galectin-3 *in vivo* by using siRNA was assessed by immunohistochemistry (Fig. 5*a*) and real-time PCR (Fig. 5*b*). siRNA treatment resulted in a significant decrease in Galectin-3 expression (Fig. 5*b*) (*P* < 0.01). Furthermore, a significant reduction in α-SMA expression was observed in Galectin-3

siRNA-treated animals relative to duplex controls (Fig. 5*b*) (*P* < 0.01). siRNA was well tolerated and no side effects were noted in the treated animals. These data demonstrate that Galectin-3 siRNA can block HSC activation in response to liver injury *in vivo*, confirming that Galectin-3 up-regulation is a key mechanism in HSC activation *in vivo* and in the pathogenesis of liver fibrosis.

Discussion

We have shown a fundamental role for Galectin-3 in the regulation of HSC activation *in vitro* and *in vivo*, thereby identifying Galectin-3 as a potential therapeutic target in the treatment of liver fibrosis. Our human biopsy data demonstrate that Galectin-3 expression is increased in human liver fibrosis secondary to diverse types of injury, ranging from viral-mediated (hepatitis B and C) to metabolic disease (iron overload). This finding suggests that Galectin-3 up-regulation is a basic response within the liver regardless of the initiating agent or disease process. The pattern of Galectin-3 staining observed in the human tissue was different from the distribution observed in our animal models. This difference relates to the chronicity and intensity of the disease processes. Human tissue was taken from patients with advanced cirrhosis after years (in many cases, decades) of chronic injury and fibrosis. In our mice and rat models, a much shorter time course of injury (8 and 12 weeks, respectively) leading to liver fibrosis was examined. It seems likely that, if the animal models were allowed to run on for years, a similar pattern of fibrosis and Galectin-3 expression would be observed.

In our experimental model of liver fibrosis, there was a very close spatial and temporal relationship between Galectin-3 expression, myofibroblast activation, and collagen deposition. *Galectin-3* can be considered an immediate early gene and is up-regulated rapidly in response to tissue injury (37, 38). Our results demonstrate that spontaneous HSC activation occurs in WT but not *Galectin-3$^{-/-}$* HSCs, and that this defect can be overcome by exogenous addition of Galectin-3 (which is rapidly internalized by HSCs). Spontaneous activation of WT HSCs was blocked by siRNA knockdown of Galectin-3 expression. These results suggest that Galectin-3 autocrine stimulation of HSCs is sufficient for HSC activation *in vitro*. However, the perisinusoidal orientation and long cytoplasmic processes of HSCs facilitate their interactions with neighboring cell types including other nonparenchymal cells such as Kupffer cells and sinusoidal endothelial cells and liver parenchymal cells (hepatocytes). These attributes may regulate HSC phenotype and function by facilitating both autocrine and paracrine activation of myofibroblasts by Galectin-3 by means of cell–cell contacts, cell–matrix contacts, and soluble factors. Furthermore, within the injured liver, injured epithelium (hepatocytes) up-regulate Galectin-3 expression after injury, and both recruited and resident tissue macrophages are abundant sources of Galectin-3 (39). Thus both autocrine and paracrine Galectin-3-stimulated HSC activation may exist during liver inflammation and fibrosis *in vivo*.

TGF-β is a major profibrogenic cytokine and is a key mediator of fibrosis in many different organs (31). TGF-β mRNA expression was markedly elevated after hepatic injury; however, expression of TGF-β was similar in whole liver homogenates from fibrotic liver in WT and *Galectin-3$^{-/-}$* mice. Secretion of TGF-β was the same in WT and *Galectin-3$^{-/-}$* macrophages and HSCs, and Smad-2 and Smad-3 signaling in HSCs was similar between the two genotypes when stimulated with TGF-β. However, despite similar levels of TGF-β and intact TGF-β signaling pathways, the absence of Galectin-3 markedly inhibited the fibrotic phenotype *in vitro* and *in vivo* in our animal model. These data demonstrate that TGF-β stimulated HSC activation and procollagen production requires Galectin-3.

Galectin-3 can form pentamers in the presence of multivalent ligands, cross-linking glycoproteins at the cell membrane (40). The resultant superstructure of galectins and glycoproteins at the cell surface can bind cell–surface receptors such as the epidermal growth factor receptor (41), regulating receptor activation and intracellular signaling. Our time course experiments examining trafficking of exogenous recombinant Galectin-3 added to primary HSCs suggest that Galectin-3 is rapidly internalized. Furthermore, siRNA-mediated knockdown of Galectin-3 inhibited myofibroblast activation and procollagen expression. Intracellularly, Galectin-3 can shuttle between the nucleus and the cytoplasm (42) and is involved in fundamental processes such as pre-mRNA splicing (43, 44), cell-cycle progression (45, 46), proliferation (11, 12, 47), and apoptosis (16, 17, 48, 49) mainly through intracellular protein–protein interactions rather than lectin–carbohydrate interactions. However the precise mechanisms by which Galectin-3 regulates these intracellular processes still have to be defined. Recently, it has been shown that TGF-β can induce renal fibrosis in a Smad-2/-3-independent fashion (50, 51) and activates additional signaling molecules such as p38 (52), bcr-abl (51), and PAK2 (53). Our results suggest that TGF-β requires intracellular Galectin-3 to stimulate myofibroblast activation and procollagen production independent of Smad-2 and Smad-3.

RNA interference allows indepth study of the molecular mechanisms of disease through specific gene target inhibition. Furthermore, siRNAs hold direct therapeutic promise, as agents capable of attenuating the expression of disease-causing genes (54). We used siRNA duplexes to specifically examine the role of Galectin-3 in myofibroblast activation and liver fibrosis *in vitro* and *in vivo*. siRNA silencing of Galectin-3 expression in both primary mouse and human HSCs resulted in inhibition of myofibroblast activation and procollagen (I) expression. Multiple duplexes were used for silencing experiments to ensure that target knockdown correlated with the observed functional outcomes. siRNA knockdown of Galectin-3 *in vivo* reduced myofibroblast activation in our model of hepatic injury. Thus, Galectin-3 is critical for myofibroblast activation *in vivo*. Strategies to knockdown expression of Galectin-3 in the liver may lead to the development of alternative antifibrotic therapies.

Materials and Methods

Materials. Cytokines and recombinant mouse Galectin-3 were purchased from R & D Systems and PeproTech EC (London, U.K.). All other reagents were from Sigma-Aldrich unless otherwise stated.

Animals. Generation of *Galectin-3$^{-/-}$* mice by gene-targeting technology has been described in ref. 18. As controls, age- and sex-matched WT littermate mice were used. All procedures were undertaken with approved license from the Animal Scientific Procedures Division of the Home Office (London, U.K.).

CCL$_4$-Induced Liver Injury Models. *Acute.* After overnight fast (with free access to water) mice were injected i.p. with 1 μl/g body weight sterile CCL$_4$ in a 1:3 ratio with olive oil or olive oil (control). Livers were harvested for analysis at 24, 48, 72, 96, and 168 h.
Chronic CCL$_4$-induced liver fibrosis. Mice were injected i.p. with 1 μl/g body weight sterile CCL$_4$ in a 1:3 ratio with olive oil or olive oil (control) twice weekly for 8 weeks. The rat model of CCL$_4$-induced liver fibrosis was undertaken as described in ref. 26.

Immunohistochemistry. Paraffin-embedded sections of liver were processed for immunohistochemistry and immunofluoresence as described in refs. 27 and 29. See *Supporting Materials and Methods* for details of primary antibodies used. Tissue fibrosis was visualized and quantified with a PSR stain as described (26). Morphometric measurements were made on 10-μm sections stained with PSR by using OPENLAB software (Improvision, Coventry, U.K.). Forty random fields from each section were analyzed at a final magnification of ×100. Each captured field was analyzed by separation into red, green, and blue (RGB) filters, and the red area was mathematically divided by the RGB area and multiplied by 100%. This

calculation represents the percentage area staining positively for collagen fibers, providing a quantitative value on a continuous scale.

HSCs Extraction, Culture, and Growth. Primary human and mouse HSCs were isolated and passaged exactly as described in refs. 26 and 27. Primary mouse HSCs were seeded at a density of 5,000 cells per well in 96-well plates, and proliferation measured by using 3-(4,5-dimethylthiazol-2-yl)-2,5-diphenyl tetrazolium bromide formazan production (Sigma).

Western Blotting. Western blot analysis was undertaken by using the following primary antibodies: anti-α-SMA clone 1A4 (Sigma), anti-Galectin-3 clone A3A12 (Alexis Biochemicals, Nottingham, U.K.), anti-Smad-2 and -3 [BioSource (Paisley, U.K.) and Invitrogen], anti-phospho-extracellular signal-regulated kinase 1/2 (Sigma), anti-phospho-PKC (Cell Signaling Technology, Beverly, MA).

Real-Time PCR. Total RNA from whole liver was reverse transcribed into cDNA (Applied Biosystems). See *Supporting Materials and Methods* for details of real-time primer sequences used.

Preparation of siRNAs and siRNA Treatment *in Vitro* and *in Vivo*. siRNAs were synthesized by using 5′-silyl-2′-tris (acetoxyethyl) orthoformate method (Dharmacon Research). See *Supporting Materials and Methods* for details of siRNA sequences used.

In vitro. Subconfluent cultures of primary mouse and human HSCs in 6-well plates were transfected with siRNA (final concentration, 250 nM) by using oligofectamine (Invitrogen). After 96 h, cells were lysed for protein or RNA extraction.

In vivo. After overnight fast (with free access to water), mice were injected i.p. with 1 μl/g body weight sterile CCL$_4$ in a 1:3 ratio with olive oil. Animals were anaesthetized 2 hours later, and a cannula was inserted into the portal vein. Fifty micrograms of Galectin-3 siRNA (Duplex no. 2, siSTABLE; Dharmacon) in 300 μl PBS was rapidly delivered via the portal vein (2 mg/kg). Before removal of the cannula, Gelaspon (Johnson & Johnson, Maidenhead, U.K.) was applied to the portal vein to prevent bleeding. Further delivery of Galectin-3 siRNA at 24 and 48 h was by rapid hydrodynamic tail vein injection (50 μg of siRNA in 1 ml PBS). Control mice received PBS or siCONTROL nontargeting siRNA no. 2 (Dharmacon) by the same routes. Mice were anaesthetised on day 3 ($n = 6$ in each group), and liver tissue was fixed in buffered formalin, whereas the remaining liver was snap-frozen for protein and mRNA analysis.

Statistical Analysis. Results are presented as mean $\pm$ SEM. Significance of the differences between means was assessed by using one-way analysis of variance (ANOVA) or two-tailed Student's t test. Values of $P < 0.05$ were considered significant. Unless stated otherwise, studies were performed on three to six independent occasions.

1. Neuberger, J. (2000) *J. Hepatol.* **32,** 198–207.
2. Simpson, K. J. & Garden, O. J. (1999) *Proc. R. Coll. Physicians Edinb.* **29,** 144–152.
3. Friedman, S. L. (2000) *J. Biol. Chem.* **275,** 2247–2250.
4. Bataller, R. & Brenner, D. A. (2005) *J. Clin. Invest.* **15,** 209–218.
5. Barondes, S. H., Castronovo, V., Cooper, D. N., Cummings, R. D., Drickamer, K., Feizi, T., Gitt, M. A., Hirabayashi, J., Hughes, C., Kasai, K., *et al.* (1994) *Cell* **76,** 597–598.
6. Barondes, S. H., Cooper, D. N., Gitt, M. A. & Leffler, H. (1994) *J. Biol. Chem.* **269,** 20807–20810.
7. Kasai, K. & Hirabayashi, J. (1996) *J. Biochem. (Tokyo)* **119,** 1–8.
8. Rabinovich, G. A., Baum, L. G., Tinari, N., Paganelli, R., Natoli, C., Liu, F. T. & Iacobelli, S. (2002) *Trends Immunol.* **23,** 313–320.
9. Liu, F. T. (1990) *Crit. Rev. Immunol.* **10,** 289–306.
10. Mehul, B. & Hughes, R. C. (1997) *J. Cell Sci.* **110,** 1169–1178.
11. Moutsatsos, I. K., Wade, M., Schindler, M. & Wang, J. L. (1987) *Proc. Natl. Acad. Sci. USA* **84,** 6452–6456.
12. Inohara, H., Akahani, S. & Raz, A. (1998) *Exp. Cell Res.* **245,** 294–302.
13. Kuwabara, I. & Liu, F. T. (1996) *J. Immunol.* **156,** 3939–3944.
14. Inohara, H. & Raz, A. (1995) *Cancer Res.* **55,** 3267–3271.
15. Inohara, H., Akahani, S., Koths, K. & Raz, A. (1996) *Cancer Res.* **56,** 4530–4534.
16. Yang, R. Y., Hsu, D. K. & Liu, F. T. (1996) *Proc. Natl. Acad. Sci. USA* **93,** 6737–6742.
17. Akahani, S., Nangia-Makker, P., Inohara, H., Kim, H. R. & Raz, A. (1997) *Cancer Res.* **57,** 5272–5276.
18. Colnot, C., Ripoche, M. A., Milon, G., Montagutelli, X., Crocker, P. R. & Poirier, F. (1998) *Immunology* **94,** 290–296.
19. Hsu, D. K., Yang, R. Y., Pan, Z., Yu, L., Salomon, D. R., Fung-Leung, W. P. & Liu, F. T. (2000) *Am. J. Pathol.* **156,** 1073–1083.
20. Strieter, R. M. & Keane, M. P. (2004) *J. Clin. Invest.* **114,** 165–168.
21. Hsu, D. K., Dowling, C. A., Jeng, K. C., Chen, J. T., Yang, R. Y. & Liu, F. T. (1999) *Int. J. Cancer* **81,** 519–526.
22. Wang, L., Friess, H., Zhu, Z., Frigeri, L., Zimmermann, A., Korc, M., Berberat, P. O. & Buchler, M. W. (2000) *Lab. Invest.* **80,** 1233–1241.
23. Kasper, M. & Hughes, R. C. (1996) *J. Pathol.* **179,** 309–316.
24. Maeda, N., Kawada, N., Seki, S., Arakawa, T., Ikeda, K., Iwao, H., Okuyama, H., Hirabayashi, J., Kasai, K. & Yoshizato, K. (2003) *J. Biol. Chem.* **278,** 18938–18944.
25. Sasaki, S., Bao, Q. & Hughes, R. C. (1999) *J. Pathol.* **187,** 481–489.
26. Issa, R., Zhou, X., Constandinou, C. M., Fallowfield, J., Millward-Sadler, H., Gaca, M. D., Sands, E., Suliman, I., Trim, N., Knorr, A., *et al.* (2004) *Gastroenterology* **126,** 1795–1808.
27. Iredale, J. P., Benyon, R. C., Pickering, J., McCullen, M., Northrop, M., Pawley, S., Hovell, C. & Arthur, M. J. (1998) *J. Clin. Invest.* **102,** 538–549.
28. Gressner, A. M. (1996) *Kidney Int. Suppl.* **54,** S39–S45.
29. Duffield, J. S., Forbes, S. J., Constandinou, C. M., Clay, S., Partolina, M., Vuthoori, S., Wu, S., Lang R. & Iredale J. P. (2005) *J. Clin. Invest.* **115,** 56–65.
30. Imamura, M., Ogawa, T., Sasaguri, Y., Chayama, K. & Ueno, H. (2005) *Gastroenterology* **128,** 138–146.
31. Leask, A. & Abraham, D. J. (2004) *FASEB J.* **18,** 816–827.
32. Uemura, M., Swenson, E. S., Gaca, M. D., Giordano, F. J., Reiss, M., Wells, R. G. (2005) *Mol. Biol. Cell* **16,** 4214–4224.
33. Qi, Z., Atsuchi, N., Ooshima, A., Takeshita, A. & Ueno, H. (1999) *Proc. Natl. Acad. Sci. USA* **96,** 2345–2349.
34. Kaviratne, M., Hesse, M., Leusink, M., Cheever, A. W., Davies, S. J., McKerrow, J. H., Wakefield, L. M., Letterio, J. J. & Wynn, T. A. (2004) *J. Immunol.* **173,** 4020–4029.
35. Rodriguez-Vita, J., Sanchez-Lopez, E., Esteban, V., Ruperez, M., Egido, J., Ruiz-Ortega, M. (2005) *Circulation* **111,** 2509–2517.
36. Heldin, C. H., Miyazono, K. & ten Dijke, P. (1997). *Nature* **390,** 465–471.
37. Kadrofske, M. M., Openo, K. P. & Wang, J. L. (1998) *Arch. Biochem. Biophys.* **349,** 7–20.
38. Chiariotti, L., Salvatore, P., Frunzio, R. & Bruni, C. B. (2004) *Glycoconj. J.* **19,** 441–449.
39. Sato, S. & Hughes, R. C. (1994) *J. Biol. Chem.* **269,** 4424–4430.
40. Ahmad, N., Gabius, H. J., Andre, S., Kaltner, H., Sabesan, S., Roy, R., Liu, B., Macaluso, F. & Brewer, C. F. (2004) *J. Biol. Chem.* **279,** 10841–10847.
41. Partridge, E. A., Le Roy, C., Di Guglielmo, G. M., Pawling, J., Cheung, P., Granovsky, M., Nabi, I. R., Wrana, J. L., Dennis, J. W. (2004) *Science* **306,** 120–124.
42. Davidson, P. J., Davis, M. J., Patterson, R. J., Ripoche, M. A., Poirier, F. & Wang, J. L. (2002) *Glycobiology* **12,** 329–337.
43. Dagher, S. F., Wang, J. L. & Patterson, R. J. (1995) *Proc. Natl. Acad. Sci. USA* **92,** 1213–1217.
44. Wang, J. L., Gray, R. M., Haudek, K. C. & Patterson, R. J. (2004) *Biochim. Biophys. Acta* **1673,** 75–93.
45. Kim, H. R., Lin, H. M., Biliran, H. & Raz, A. (1999) *Cancer Res.* **59,** 4148–4154.
46. Lin, H. M., Pestell, R. G., Raz, A. & Kim, H. R. (2002) *Oncogene* **21,** 8001–8010.
47. Shimura, T., Takenaka, Y., Tsutsumi, S., Hogan, V., Kikuchi, A. & Raz, A. (2004) *Cancer Res.* **64,** 6363–6367.
48. Honjo, Y., Nangia-Makker, P., Inohara, H. & Raz, A. (2001) *Clin. Cancer Res.* **7,** 661–668.
49. Yu, F., Finley, R. L., Jr., Raz, A. & Kim, H. R. (2002) *J. Biol. Chem.* **277,** 15819–15827.
50. Moustakas, A. & Heldin, C. H. (2005) *J. Cell Sci.* **118,** 3573–3584.
51. Wang, S., Wilkes, M. C., Leof, E. B. & Hirschberg, R. (2005) *FASEB J.* **19,** 1–11.
52. Tsukada, S., Westwick, J. K., Ikejima K., Sato N. & Rippe R. A. (2005) *J. Biol. Chem.* **280,** 10055–10064.
53. Wilkes, M. C., Murphy, S. J., Garamszegi, N. & Leof, E. B. (2003). *Mol. Cell. Biol.* **23,** 8878–8889.
54. Soutschek, J., Akinc, A., Bramlage, B., Charisse, K., Constien, R., Donoghue, M., Elbashir, S., Geick, A., Hadwiger, P., Harborth, J., *et al.* (2004) *Nature* **432,** 173–178.

MEDICAL SCIENCES